Sensors and Actuators B 263 (2018) 445–451

Contents lists available at ScienceDirect

Sensors and Actuators B: Chemical

journal homepage: www.elsevier.com/locate/snb

High performance mixed-potential-type Zirconia-based NO_2 sensor with self-organizing surface structures fabricated by low energy ion beam etching

Rui You [a], Xidong Hao [b], Hongyan Yu [a], Baoxu Wang [b], Geyu Lu [b], Fangmeng Liu [b,*], Tianhong Cui [c,*]

[a] Department of Precision Instrument, Tsinghua University, Beijing, 100084, China
[b] State Key Laboratory on Integrated Optoelectronics, College of Electronic Science and Engineering, Jilin University, 2699 Qianjin Street, Changchun, 130012, China
[c] Department of Mechanical Engineering, University of Minnesota, Minneapolis, MN, 55455, USA

ARTICLE INFO

Article history:
Received 14 November 2017
Received in revised form 22 January 2018
Accepted 13 February 2018
Available online 19 February 2018

Keywords:
NO_2 sensing
Yttria-stabilized-zirconia
Ion beam etching
Self-organized nanostructure
Mixed-potential

ABSTRACT

The mixed-potential-type NO_2 sensor based on a yttria-stabilized zirconia (YSZ) electrolyte with NiO sensing electrode and a three-phase boundary (TPB) was fabricated. The ion beam etching (IBE) technology with low energy was employed to etch the YSZ substrate for the first time. The characterization result indicates that the YSZ substrate prepared by argon ion (Ar^+) beam with different incident angles (10° and 40°) obtains hollow and spike patterns on the surface, respectively. The sensing performance was improved by the self-organized nanostructures of TPB, which enhances the contact area obviously. The sensor using a YSZ substrate processed by 10° incident angle with 800 eV/60 mA energy demonstrates the largest response compared with other parameters to NO_2 at 850 °C. Sensitivity of the sensors is achieved as 40.7 mV/decade, about 1.9 times as the initial YSZ substrate. In addition, the sensor also has good response-recovery transients, repeatability and selectivity.

© 2018 Elsevier B.V. All rights reserved.

1. Introduction

Air pollution has caused many global environmental disasters and harmed people's health in our daily life due to the rapid development of the fertilizer, automobile and industries [1,2]. In particular, nitrogen oxides gases (NO_x) from vehicles exhaust as mainly harmful gas pollutants, causing a variety of adverse health factors and some urban atmosphere pollution problems [3]. To continuously monitor and detect the NO_x from car exhaust accurately and precisely, 8 mol% Y_2O_3-doped ZrO_2 (YSZ-8Y) based mix-potential-type (MPT) NO_x sensor is one of the most investigated devices applied to vehicle emission systems, because of its high operation temperatures and excellent chemical and thermal stability [4–7].

To improve the sensing performance of the YSZ NO_x sensor, research was focused on developing new composite materials and the microstructure of sensing electrode [8–13]. Recently, there is research to show that the modified structure of three-phase boundary (TPB) is another important factor to improve the performance of sensors. For example, Liang et al. developed YSZ-substrate with rough surface by hydrofluoric acid chemical corrosion method [14]. Guan et al. enlarged the area of TPB by femtosecond laser direct writing technology [15]. Yin et al. fabricated a high performance sensor by using a porous double-layer YSZ substrate with large surface area [16]. Liu et al. formed different three-dimensional TPB by mixed YSZ particles with $Co_3V_2O_8$ material as a sensing electrode [17]. Wang et al. constructed well-ordered TPB with a pore array with nanostructures by template method with self-assembled polystyrene spheres [18]. Low energy ion beam etching (IBE) technology is the latest progress of fabrication to create large area microstructures with the advantages of efficient, low cost, high processing precision and little damage to the sample surface [19–21].

In this work, for the first time, the low energy IBE technology (800 eV/60 mA) was used to process the micro hollow and spike structure on the surface of YSZ- substrate. The high performance MPT sensor based on NiO sensing electrode and modified YSZ solid electrolyte was developed and utilized to detect NO_2. The detailed sensing properties and sensing mechanism were investigated.

* Corresponding authors.
E-mail addresses: liufangmeng@jlu.edu.cn (F. Liu), tcui@me.umn.edu (T. Cui).

https://doi.org/10.1016/j.snb.2018.02.104
0925-4005/© 2018 Elsevier B.V. All rights reserved.

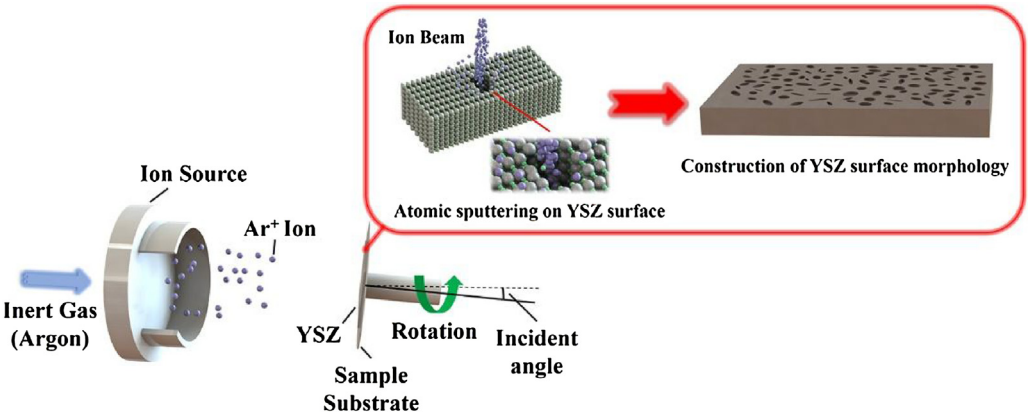

Fig. 1. Schematic of argon ion beam etching process.

2. Experimental

As shown in Fig. 1, the YSZ ceramic substrate (YSZ-8Y, $2 \times 2 \times 0.3\,mm^3$, Anpeisheng Corp., China) was fabricated by the ion beam etching system (IBED-70, RUIDEGAOER Technology Co. Ltd, China). The YSZ substrate was cleaned and fixed on a sample stage of sputtering cavity by silica gel changing the incident angle from 0° to 90°. The surface of YSZ was processed by two groups of parameters with different incident angles (10° and 40°) for 90 min. The energy transferred from incident ion (Ar^+) to target atoms (YSZ), resulting in the substrate material removal and sputtering roughening. In this case, variety of nanostructures were formed, such as hollow, stripe and spike patterns [22–26].

The NiO nanoparticles were synthesized by coordination homogeneous precipitation method [27]. Firstly, 0.2 mol/L $NiCl_2$ solution was obtained by dissolved $NiCl_2{\cdot}6H_2O$ into deionized water. Then, ammonia and deionized water were mixed by the volume ratio of 1: 10 to achieve the diluted ammonia solution. After 60 min stirring, the $NiCl_2$ solution was placed in oil-bath at 60 °C and the ammonia solution was dropped into $NiCl_2$ solution with the rate of 6 droplets/min, the flocculent precipitates were appeared until the pH value of mixture was measured at 8. After the reaction is stopped, the precipitates were collected by centrifugation, washed with DI water and absolute ethanol for 6 times alternatively. The product was dried in an electric oven at 80 °C for 12 h and finally the green NiO nanoparticle was obtained by sintering at 1100 °C in muffle furnace.

The schematic diagram of typically MPT sensors based on a YSZ substrate with different parameters of etching method was exhibited in Fig. 2. The Pt reference electrode (RE) ($0.6 \times 2\,mm^2$) and the point-shaped platinum pad on the YSZ substrate were patterned by printing process using platinum paste (Sino-platinum Metals Co., China). To fabricate the sensing electrode (SE), the NiO powder synthesized by precipitation method was mixed to deionized water and covering the Pt pad ($1 \times 2\,mm^2$). Finally, it was sintered at 1100 °C for 3 h. In order to compare the gas sensing performance of NO_2 sensor, the device with unprocessed YSZ substrate was labeled as Sensor 0, and other treating method were defined as Sensor 1 (40°) and Sensor 2 (10°).

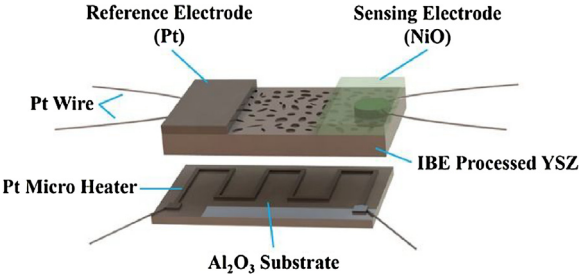

Fig. 2. Schematic diagram of a mixed-potential-type NO_2 sensor based on IBE processed YSZ substrate and NiO electrode.

The crystalline structure of NiO sensing material was characterized by X-ray diffraction (XRD) (Rigaku wide-angle X-ray diffractometer with a monochromator for Cu-Kα radiation at wave length of 0.1541 nm) in the range of 20–80° at scanning rate of 10°/min. The surface properties of the YSZ substrate processed by

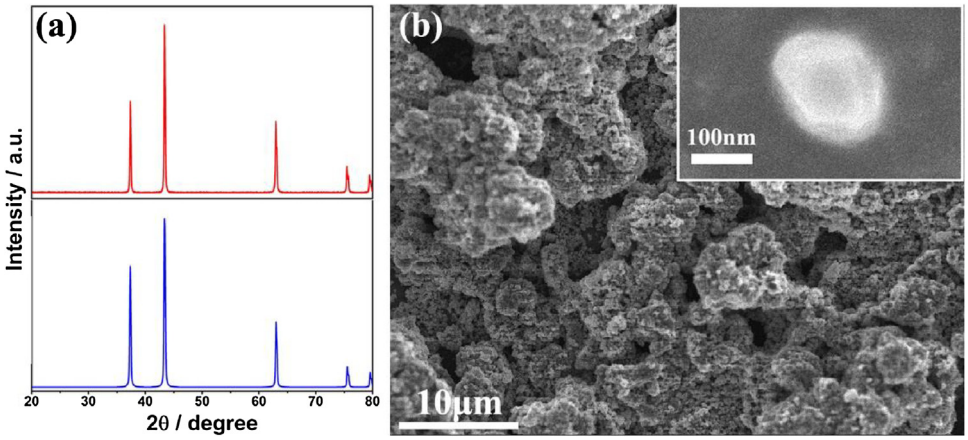

Fig. 3. (a) XRD patterns of NiO powders sintered at 1100 °C and (b) SEM image of NiO sensing electrode sintered at 1100 °C and single NiO nanoparticle (insert).

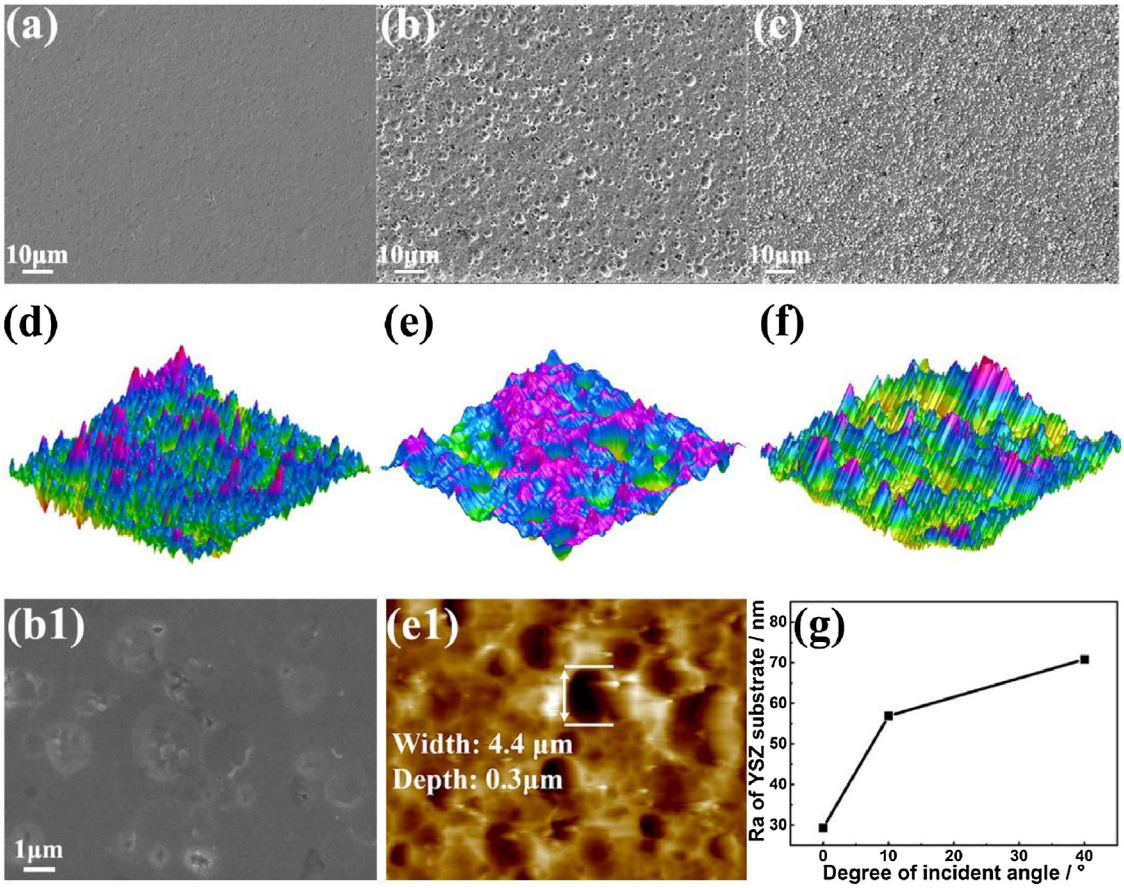

Fig. 4. (a–c) SEM images of the surface of YSZ substrate etched by different incident angles of Ar^+ beam: (a) unprocessed, (b) 10° incident angle, (c) 40° incident angle. AFM images of (d) smooth YSZ substrate and the morphology of YSZ treated with (e) 10° incident angle, (f) 40° incident angle. Microstructured characterizations of micro hollow fabricated by 10° etching angle. (b1) characterized by SEM, (e1) measured by AFM. (g) Roughness average (Ra) of the YSZ substrate processed by 10°, 40° and unprocessed, respectively.

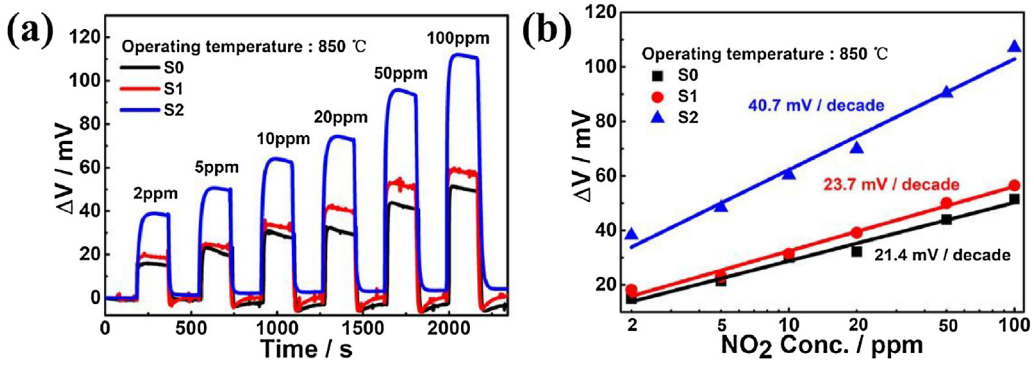

Fig. 5. (a) Response transients of the different sensors (S0-S2) to NO_2 in the range from 2 ppm to 100 ppm at 850 °C. (b) Dependence of ΔV on the logarithm of NO_2 at an NO2 concentration from 2 to 100 ppm of S0-S2.

IBE technology were characterized by field emission scanning electron microscope (JEOL JSM-6500F) and atomic force Microscope (AFM; Being Nano-Instrument, Ltd., CSPM5500, China).

The NO_2 sensing performance was performed in a statics measurement method[11], which powered by a DC power supply (GPD-3303S, GWINSTEK, China). The NO_2 sensor was measured in an airtight chamber with the relative humidity of 25% and environment temperature of 26 °C. The digital electrometer (8846A, FLUKE, USA) was used to monitor the potential difference (ΔV) between SE and RE. The response time of the sensor exposed to air and different concentrations of NO_2 gas were uniformly set to 3 min. And the response value achieved at last second in gas was used as the potential value for the calibration curves to ensure the accuracy of the test. The working temperature of NO_2 sensors was obtained and calibrated by infrared imaging camera (T250, FLIR, USA).

3. Results and discussion

XRD patterns of NiO sensing material sintered at 1100 °C for 3 h were shown as Fig. 3a. All main peaks can be indexed to the standard NiO structure (JCPDS# 75–179) without other impurities, suggesting the high crystallization of the oxide material. The

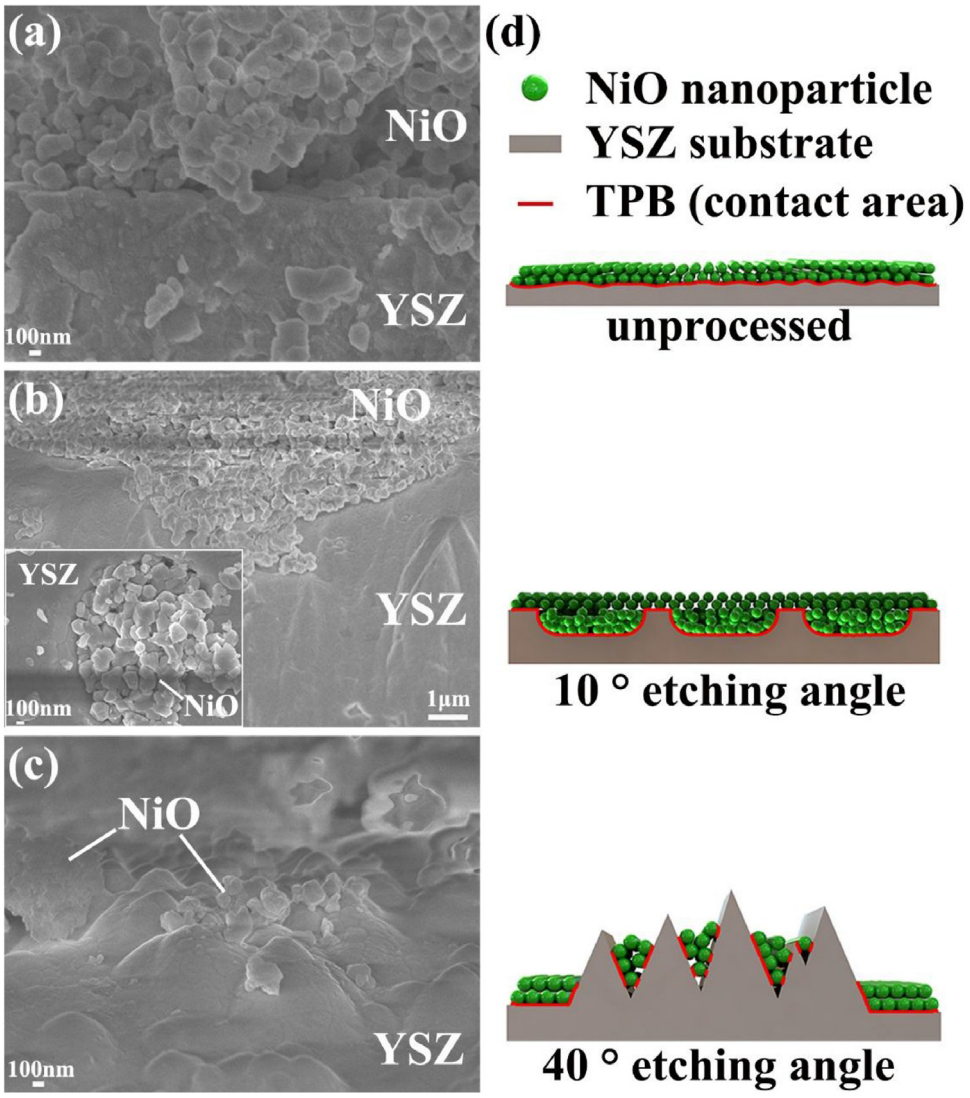

Fig. 6. The cross section SEM images of NiO/YSZ surface structure processed by different etching method of (a) unprocessed, (b) 10° etching angle and (c) 40° etching angle. (d) Schematic diagram of different three-phase boundaries (TPB) based on YSZ substrate and NiO nanoparticles.

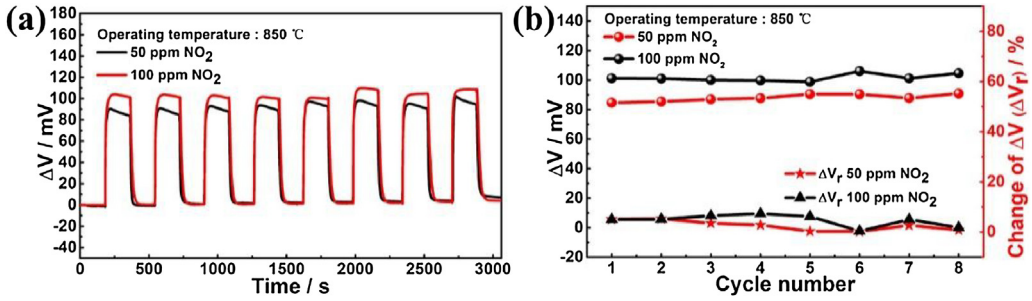

Fig. 7. (a) Response-recovery transients of sensor S2 to 50 and 100 ppm NO_2 at operating temperature of 850 °C. (b) Continuous stability of sensor S2 to 50 and 100 ppm NO_2 for 8 alternative cycles at 850 °C.

surface topography of NiO sensing electrode was characterized as Fig. 3**b**. As shown in insert image, the diameter of NiO nanoparticle is about 100 nm. The diffusion of the NO_2 was benefited from such porous and loose nanostructures of NiO sensing electrode.

The surface profiles of the YSZ substrate processed by IBE were characterized by SEM and AFM, as shown in Fig. 4. Fig. 4a indicates the primary morphology of the YSZ substrate surface without IBE process. Fig. 4b–c shows the surface of YSZ substrate fabricated by incident angles of 10° and 40°, respectively. The surface topography of YSZ substrate was changed by IBE processed obviously. The micro hollow and pore structures appeared with 10° etching angle randomly and dispersedly, and the spike structures were distributed with 40° etching angle uniformly. The micro hollow structures processed by IBE technology with several microns were shown in Fig. 4b. AFM was used to characterize the microstructure and the roughness of YSZ substrate surface in details. As shown in Fig. 4d–f,

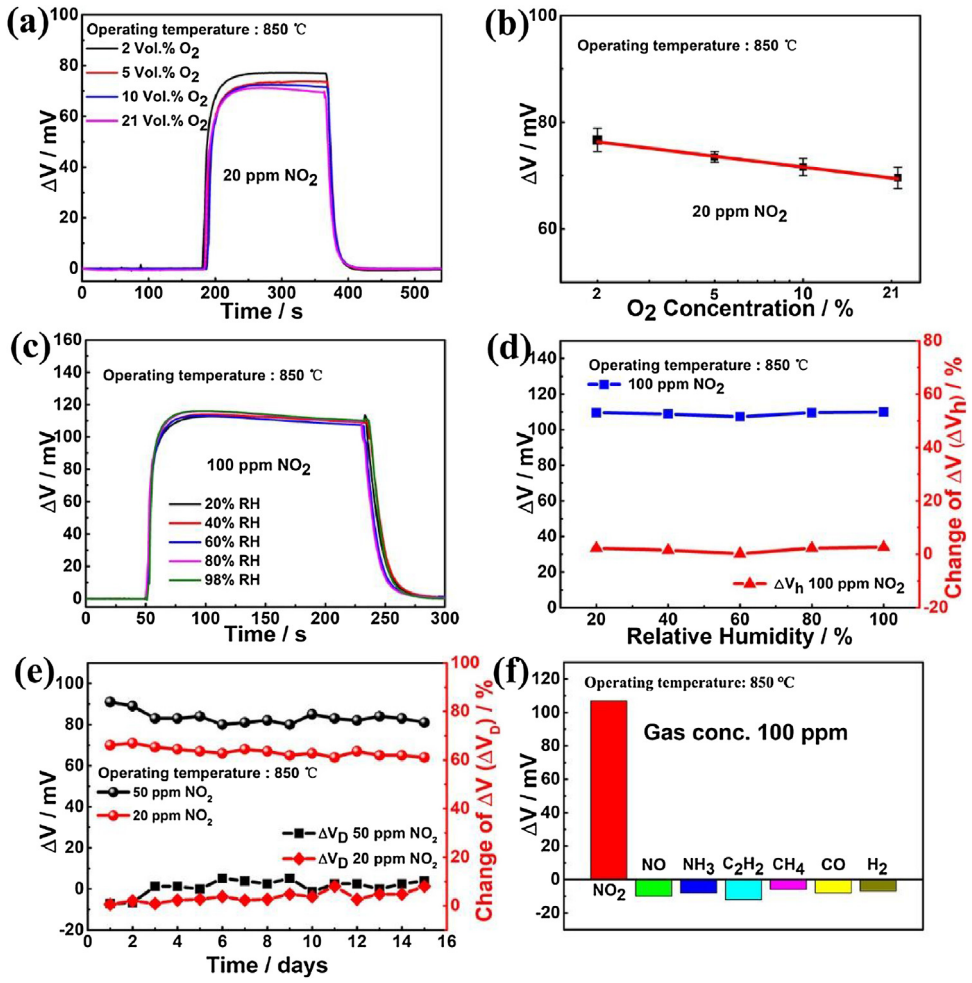

Fig. 8. (a) Response and recovery curves of sensor S2 to 20 ppm NO_2 at various concentrations of O_2 at 850 °C. (b) Dependence of ΔV for sensor S2 to 20 ppm NO_2 on the logarithm of different concentrations of O_2. (c) Responses of sensor S2 to 100 ppm NO_2 under relative humidity from 2% to 98% at 850 °C. (d) Stability of sensor S2 to 100 ppm NO_2 for under different relative humidity. (e) Long-term stability of sensor S2 to 20 and 50 ppm NO_2 for 15 days. (f) Selectivity of the sensor utilizing NiO sensing electrode material sintered at 1100 °C to various gases at the working temperature of 850 °C.

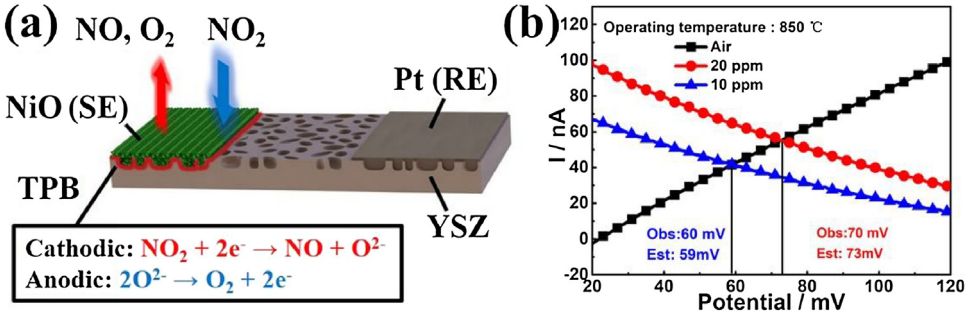

Fig. 9. (a) Schematic view of the mechanism of MPT NO_2 sensor fabricated by NiO (SE) and IBE processed YSZ substrate. (b) Polarization curves in air, 10 ppm and 20 ppm NO_2 for sensor S2 at 850 °C.

three-dimensional (3D) graph of YSZ surface processed by different etching angles was measured by AFM. Different structure of YSZ surface can be analyzed obviously, and the characterization result was matched with the SEM. Furthermore, the geometry (width and depth) of the hollow structure was given by NanoScope Analysis software precisely, as indicated in Fig. 4e1. Fig. 4g gives the roughness average (Ra) of the YSZ substrate surface with unprocessed and two different etching methods. It is obvious that with the increase of incident angle, the roughness of YSZ is increased notably. Recently, our research indicates that large roughness averages especially the porous structures would construct a better three-phase boundary of YSZ sensors [14,18,28]. It may be explained as more active sites of oxidation-reduction reaction were created by the larger contact area between the sensing electrode material and the YSZ substrate surface. Hence, we consider that the large roughness averages of modified TPB processed by IBE method will increase the response of NO_2 of YSZ sensor.

As demonstrated in Fig. 5, transient response of the NO_2 sensors with unprocessed YSZ substrate (S0) and sensor S1, S2 were tested at a concentration gradient from 2 to 100 ppm NO_2. The operating

temperature of sensor S0, S1 and S2 was set at 850 °C which was tested and proved to be the optimal operation temperature of NiO material in our published report [14,18,28]. As shown in Fig. 5a, response value of electric potential difference (ΔV) was improved by increase of Ra of YSZ substrates. In addition, the response of sensor S2 to 100 ppm NO_2 was 106.5 mV, which was 1.7 times as sensor S0 (64.3 mV) significantly. However, the response of sensor S1 was increased 7% compared to sensor S0 approximately. As indicated in Fig. 5b, the ΔV is linearly dependent on the logarithm of NO_2 concentration in detected range, which conformed to the mixed-potential mechanism. The slop of sensor S0, S1 and S2 were derived as 21.4, 23.7 and 40.7 mV/decade, respectively. Sensor S2 using the YSZ substrate etched by 10° incident angle achieved the best slope, about 1.9 times as unprocessed YSZ sensor.

However, it is noted that the above results were not completely consistent with previous studies. The response of sensor S1 is far less than that of sensor S2, though it had the largest roughness average of YSZ surface. This is because the contact area of TPB was not only depended on the roughness of substrate surface, but also considered to the structure matching degree between the YSZ substrate and the sensing electrode material. High resolution SEM images of different NiO/YSZ surface structure were indicated in Fig. 6. As shown in Fig. 6a, the NiO electrode material was combined with the flat YSZ substrate. The continuous planar contacts were formed between NiO nanoparticles and solid electrolyte. Compared with the flat structure, as exhibited in Fig. 6b, the NiO nanoparticles fabricated on YSZ substrate could be easily embedded into the hollow structure processed by 10° etching angle, which obviously enlarged the contact area (TPB) between sensing electrode and YSZ substrate. It can be seen from Fig. 6c that the NiO nanoparticles were placed on the fabricated spike shaped structures. Although the spike shaped structures fabricated by 40° etching angle provided the largest surface roughness, the rugged and dense surface structure greatly reduced the matching degree of NiO nanoparticles and the surface of YSZ as demonstrated in Fig. 6d. Compared with the flat and spike structures, the hollow structures with NiO nanoparticles achieved the largest contact area of TPB and the best of matching degree effectively. Thus the response of NO_2 sensor S2 was evidently increased by the IBE processed YSZ substrate with 10° etching angle. The above conclusion was discovered and discussed in our research previously [29].

The response-recovery transients of sensor S2 are demonstrated in Fig. 7a with 8 alternative cycles to 50 and 100 ppm NO_2 at 850 °C. Fig. 7b illustrates the ΔV of each concentration at each time during experiment specifically. The ΔV_r (the change of ΔV, $\Delta V_r = [\Delta V_n - \Delta V_0/\Delta V_0 \times 100\%]$, where ΔV_0 and ΔV_n represent the ΔV of the sensor in Fig. 5 and the nth measurement) are less than 5% and 7% to 50 ppm and 100 ppm, respectively. These result exhibits good repeatability performance of NO_2 sensor.

According to the mixed-potential model, the sensor response affected by a variation of oxygen concentration [30,31]. Fig. 8a exhibits the response transient of sensor S2 to 20 ppm NO_2 mixing to 2%, 5%, 10% and 21% O_2, respectively. The ΔV was linear to the logarithm of the oxygen concentration with a negative slope, as shown in Fig. 8b. This phenomenon not only follows search conclusions of predecessors, but also proves that the NO_2 sensor was corresponded to the typical mixed-potential mechanism. Moreover, the influence of moisture and long-term stability of sensor S2 were also investigated. As presented in Fig. 8c, the response of sensor S2 based on NiO sensing material to 100 ppm NO_2 was tested in the relative humidity (RH) in the range of 20–98% at 850 °C, respectively. Fig. 8d gives the ΔV_h (the change of ΔV, $\Delta V_h = [\Delta V_n - \Delta V_0/\Delta V_0 \times 100\%]$, where ΔV_0 and ΔV_n denote the ΔV of the sensor under 15% and n% relative humidity) of sensor S2 to 100 ppm NO_2 is less than 3.2%, demonstrating a good humidity resistance of sensor. In addition, 15 days' long-term stability of sensor S2 with the concentration of 20 ppm and 50 ppm was discussed, as shown in Fig. 8e. The result indicates that the change of ΔV of sensor S2 is less than 4.8% and 11.3%, respectively. As shown in Fig. 8f, sensor S2 fabricated by the IBE process with 10° incident angle also exhibits good selectivity to NO_2 between various of gas pollution from the automobile's exhaust, such as NO, NH_3, CO, CH_4 and C_2H_2 to the concentration of 50 ppm at 850 °C.

The mechanism of mixed-potential-type (MPT) NO_2 sensor was proposed by Lu et al., reported in our previous work [5,11,32]. The sensor we developed can be described by the electrochemical cells. When the sensor is exposed to NO_2, there are two electrochemical reactions taking place at the TPB, as described in Fig. 9a. The sensing mechanism was testified by the modified polarization curves corresponding to the cathodic and anodic reactions [14,28]. Fig. 9b indicates that the modified polarization curves of sensor S2 were obtained by testing in air and the concentration of 10 and 20 ppm NO_2 with air. The anodic curve was measured in air atmosphere, and the cathodic curve was treated with the value of NO_2 with air subtract the part of air. The mixed-potential value estimated from the intersection of the cathodic and anodic polarization curves were practically coincided to the measurment value to 10 and 20 ppm NO_2, respectively. Such consistency used to verify the correctness of mixed-potential model was examined to plenty of YSZ sensors based on other sensing electrode material in our previous research.

4. Conclusion

A new YSZ based NO_2 sensor with high performance three-phase boundary (TPB) was reported. The ion beam etching (IBE) technology with low energy was used to construct morphology of YSZ substrate by different etching angles for the first time. The sensing performance of the sensor was improved by self-organized hollow structures of TPB, enhancing the contact area obviously. The response amplitude of the sensor with 10° incident angle of Ar^+ beam significantly enhanced to the concentration of 2–100 ppm NO_2 at 850 °C. Sensitivity of the sensor with processed YSZ at 10° etching angle was calculated as 40.7 mV/decade, 1.9 times as the sensor of an unprocessed YSZ substrate. Meanwhile, sensor processed by IBE also maintains good repeatability, selectivity, moisture resistance and stability to NO_2.

Acknowledgements

This work was financially supported by the Open Fund of the State Key Laboratory on Integrated Optoelectronics (Grant No. IOSKL2017KF09) and the State Key Laboratory of Precision Measurement Technology and Instruments, Tsinghua University. The authors also thank the State Key Laboratory on Integrated Optoelectronics, Jilin University, for the provision of fabrication and measurement service.

References

[1] R. Moos, B. Reetmeyer, A. Hürland, C. Plog, Sensor for directly determining the exhaust gas recirculation rate—EGR sensor, Sens. Actuators, B 119 (2006) 57–63.
[2] N. Miura, M. Nakatou, S. Zhuiykov, Development of NO_x sensing devices based on YSZ and oxide electrode aiming for monitoring car exhausts, Ceram. Int. 30 (2004) 1135–1139.
[3] M. Fleischer, E. Simon, E. Rumpel, H. Ulmer, Detection of volatile compounds crrelated to human diseases through analysis with chenical sensors, Sens. Actuators, B 83 (2002) 245–249.
[4] S. Fischer, R. Pohle, M. Fleischer, R. Moos, Method for reliable detection of different exhaust gas components by pulsed discharge measurements using standard zirconia based sensors, Procedia Chem. 1 (2009) 585–588.
[5] N. Miura, J. Wang, M. Nakatou, P. Elumalai, S. Zhuiykov, M. Hasei, High-temperature operating characteristics of mixed-potential-type NO_2 sensor based on stabilized-zirconia tube and NiO sensing electrode, Sens. Actuators B 114 (2006) 903–909.

[6] P.K. Sekhar, E.L. Brosha, R. Mukundan, W. Li, M.A. Nelson, P. Palanisamy, et al., Application of commercial automotive sensor manufacturing methods for NO_x/NH_3 mixed potential sensors for on-board emissions control, Sens. Actuators B 144 (2010) 112–119.
[7] T. Liu, X. Zhang, L. Yuan, J. Yu, A review of high-temperature electrochemical sensors based on stabilized zirconia, Solid State Ionics 283 (2015) 91–102.
[8] Q. Diao, C. Yin, Y. Liu, J. Li, X. Gong, X. Liang, et al., Mixed-potential-type NO_2 sensor using stabilized zirconia and Cr_2O_3–WO_3 nanocomposites, Sens. Actuators B 180 (2013) 90–95.
[9] G. Lu, Q. Diao, C. Yin, S. Yang, Y. Guan, X. Cheng, et al., High performance mixed-potential type NO_x sensor based on stabilized zirconia and oxide electrode, Solid State Ionics 262 (2014) 292–297.
[10] N. Miura, T. Sato, S.A. Anggraini, H. Ikeda, S. Zhuiykov, A review of mixed-potential type zirconia-based gas sensors, Ionics 20 (2014) 901–925.
[11] F. Liu, B. Wang, X. Yang, Y. Guan, Q. Wang, X. Liang, et al., High-temperature NO_2 gas sensor based on stabilized zirconia and $CoTa_2O_6$ sensing electrode, Sens. Actuators B 240 (2017) 148–157.
[12] K. Mahendraprabhu, P. Elumalai, Stabilized zirconia-based selective NO_2 sensor using sol-gel derived Nb_2O_5 sensing-electrode, Sens. Actuators B 238 (2017) 105–110.
[13] R. You, G. Jing, H. Yu, T. Cui, Flexible mixed-potential-type (MPT) NO_2 sensor based on an ultra-thin ceramic film, Sensors 17 (2017).
[14] X. Liang, S. Yang, J. Li, H. Zhang, Q. Diao, W. Zhao, et al., Mixed-potential-type zirconia-based NO_2 sensor with high-performance three-phase boundary, Sens. Actuators B 158 (2011) 1–8.
[15] Y. Guan, C. Li, X. Cheng, B. Wang, R. Sun, X. Liang, et al., Highly sensitive mixed-potential-type NO_2 sensor with YSZ processed using femtosecond laser direct writing technology, Sens. Actuators B 198 (2014) 110–113.
[16] C. Yin, Y. Guan, Z. Zhu, X. Liang, B. Wang, Q. Diao, et al., Highly sensitive mixed-potential-type NO_2 sensor using porous double-layer YSZ substrate, Sens. Actuators B 183 (2013) 474–477.
[17] F. Liu, Y. Guan, M. Dai, H. Zhang, Y. Guan, R. Sun, et al., High performance mixed-potential type NO_2 sensors based on three-dimensional TPB and $Co_3V_2O_8$ sensing electrode, Sens. Actuators B 216 (2015) 121–127.
[18] B. Wang, F. Liu, X. Yang, Y. Guan, C. Ma, X. Hao, et al., Fabrication of well-ordered three-phase boundary with nanostructure pore array for mixed potential-type zirconia-based NO_2 sensor, ACS Appl. Mater. Interfaces 8 (2016) 16752–16760.
[19] S. Facsko, H. Kurz, T. Dekorsy, Energy dependence of quantum dot formation by ion sputtering, Phys. Rev. B 63 (2001).
[20] B. Ziberi, F. Frost, B. Rauschenbach, T. Höche, Highly ordered self-organized dot patterns on Si surfaces by low-energy ion-beam erosion, Appl. Phys. Lett. 87 (2005) 033113.
[21] B. Ziberi, F. Frost, B. Rauschenbach, Self-organized dot patterns on Si surfaces during noble gas ion beam erosion, Surf. Sci. 600 (2006) 3757–3761.
[22] F. Frost, B. Ziberi, T. Höche, B. Rauschenbach, The shape and ordering of self-organized nanostructures by ion sputtering, Nucl. Instrum. Methods Phys. Res. Sect. B 216 (2004) 9–19.
[23] S.K. Tan, R. Liu, C.H. Sow, A.T.S. Wee, Self-organized nanodot formation on InP(100) by oxygen ion sputtering, Nucl. Instrum. Methods Phys. Res. Sect. B 248 (2006) 83–89.
[24] F. Frost, B. Ziberi, A. Schindler, B. Rauschenbach, Surface engineering with ion beams: from self-organized nanostructures to ultra-smooth surfaces, Appl. Phys. A 91 (2008) 551–559.
[25] B. Ziberi, F. Frost, M. Tartz, H. Neumann, B. Rauschenbach, Ripple rotation, pattern transitions, and long range ordered dots on silicon by ion beam erosion, Appl. Phys. Lett. 92 (2008) 063102.
[26] K. Takahiro, K. Ozaki, K. Kawatsura, S. Nagata, S. Yamamoto, K. Narumi, et al., Ion-induced self-organized ripple patterns on graphite and diamond surfaces, Appl. Surf. Sci. 256 (2009) 972–975.
[27] G. Xiao-yan, D. Jian-cheng, Preparation and electrochemical performance of nano-scale nickel hydroxide with different shapes, Mater. Lett. 61 (2007) 621–625.
[28] R. Sun, Y. Guan, X. Cheng, Y. Guan, X. Liang, J. Ma, et al., High performance three-phase boundary obtained by sand blasting technology for mixed-potential-type zirconia-based NO_2 sensors, Sens. Actuators B 210 (2015) 91–95.
[29] X. Cheng, C. Wang, B. Wang, R. Sun, Y. Guan, Y. Sun, et al., Mixed-potential-type YSZ-based sensor with nano-structured NiO and porous TPB processed with pore-formers using coating technique, Sens. Actuators B 221 (2015) 1321–1329.
[30] N. Miura, T. Raisen, G. Lu, N. Yamazoe, Highly selective CO sensor using stabilized zirconia and a couple of oxide electrodes, Sens. Actuators B (1998) 84–91.
[31] N. Miura, G. Lu, N. Yamazoe, Progress in mixed-potential type devices based on solid electrolyte for sensing redox gases, Solid State Ionics (2000) 533–542.
[32] G. Lu, N. Miura, N. Yamazoe, High-tempertaure hydrogen sensor based on stabilized zirconia and a metal oxede electrode, Sens. Actuators B (1996) 130–135.

Biographies

Rui You received his B.S. degree from Department of Opto-Electronic Engineering in 2013, Changchun University of Science and Technology, Changchun, China. He is now a Ph.D. student at the Department of Precision Instrument at Tsinghua University, Beijing, China. Currently his research interests mainly include gas sensor and application of MEMS process.

Xidong Hao received the B.Eng. degree in department of electronic science and technology in 2016. He is currently studying for his M.E. Sci. degree in College of Electronic Science and Engineering, Jilin University, China.

Hongyan Yu received the B.S. degree from Department of Software Engineering in 2014, Jiangxi Agricultural University, Nanchang, China. He works at Integrated Microsystems Laboratory in Department of Precision Instrument at Tsinghua University, Beijing, China.

Baoxu Wang received his B.E. degree in 2011 from College of Electronic Science and Engineering, Jilin University, and M.E. degree in 2014 from College of Electronic Science and Engineering, Jilin University in China. Currently he is working in State Key Laboratory on Integrated Optoelectronics, JLU Region, China.

Geyu Lu received the B.Sci. degree in electronic sciences in 1985 and the M.S. degree in 1988 from Jilin University in China and the Dr. Eng. degree in 1998 from Kyushu University in Japan. Now he is a professor of Jilin University, China. His current research interests include the development of chemical sensors and the application of the function materials.

Fangmeng Liu received his PhD degree in 2017 from College of Electronic Science and Engineering, Jilin University, China. Now he is a lecturer of Jilin University, China. His current research interests include the application of functional materials and development of solid state electrolyte gas sensor and flexible device.

Tianhong Cui is currently a Professor of Mechanical Engineering and an Affiliate Senior Member of the graduate faculty in Department of Electrical and Computer Engineering and Department of Biomedical Engineering at the University of Minnesota. He joined the faculty of the University of Minnesota in 2003. From 1995–2003, he held research or faculty positions at Tsinghua University, University of Minnesota, National Laboratory of Metrology in Japan, and Louisiana Tech University, respectively. He was a visiting professor at IMTEK, University of Freiburg in Germany in 2006, and he is holding a visiting professorship at Tsinghua University. His current research interests include MEMS/NEMS and nanotechnology for medical applications.